American Journal of Nanosciences
2021; 7(4): 59-65
http://www.sciencepublishinggroup.com/j/ajn
doi: 10.11648/j.ajn.20210704.11
ISSN: 2575-484X (Print); ISSN: 2575-4858 (Online)

Plasmon-induced Circular Dichroism and Asymmetric Hot-electrons Generation Triggered by a Chiral Molecule for Polarization-dependent Chemical Reactions

Renaud Arthur Léon Vallée

Paul Pascal Research Center, University of Bordeaux - The French National Centre for Scientific Research, Pessac, France

Email address:
renaud.vallee@crpp.cnrs.fr

To cite this article:
Renaud Arthur Léon Vallée. Plasmon-induced Circular Dichroism and Asymmetric Hot-electrons Generation Triggered by a Chiral Molecule for Polarization-dependent Chemical Reactions. *American Journal of Nanosciences.* Vol. 7, No. 4, 2021, pp. 59-65.
doi: 10.11648/j.ajn.20210704.11

Received: September 11, 2021; **Accepted**: October 5, 2021; **Published**: October 15, 2021

Abstract: Performing chiral photodetection, photocatalysis or photochemical reactions at the molecular level has always been a nearly impossible task, due to the very low efficiency of the generated optical circular dichroism signals. On the contrary, chiral colloidal nanocrystals have been shown recently to offer a very large differential response to circularly polarized light. Such a response is able to generate hot-electrons with a very strong asymmetry, thus potentially able to perform the aforementioned tasks. In this paper, an intermediate picture is chosen, for which an achiral small assembly of identical particles triggered by a chiral molecule is able to generate large plasmon-induced circular dichroism (PICD), in turn able to generate the required asymmetry in the generation rates of hot-electrons. By performing Finite Difference Time Domain simulations based on the combination of a classical model of PICD generation and a quantum-based model of hot-electrons generation, the simple design of an achiral gold NPs' dimer triggered by a chiral molecule located in the center and oriented with its transition electric dipole moment parallel to the dimer axis is shown to be able to generate a strong asymmetry in its HEs' generation response. The PICDs and related hot-electrons generation rates increase as a function of volume, surface, respectively, of the considered systems, thereby providing a way to trigger chemical reactions.

Keywords: Plasmon, Chirality, Hot Electrons, Molecule

1. Introduction

Owing notably to the concept of plasmon-induced / plasmon-coupled circular dichroism [1-7], plasmonic nanostructures have been recently designed in a wide variety of ways in order to promote the use of photovoltaic devices [8-9], solar energy conversion [10], optical sensing [11], chiral growth [12], drive photocatalytic processes [13–17] and allow efficient photodetection [17] or heat on the nanoscale [18]. Such variate applications are driven by different physical processes, which all find their roots in the electric field enhancement occurring in close proximity of the plasmonic elements. In the realm of current environmental problems, it is worth mentioning that the use of plasmonic nanostructures as photocatalytic platforms for water splitting [19], H_2 dissociation [20–23], or CO_2 reduction [24] is particularly relevant. These reactions can actually be performed by virtue of the plasmonic nanoparticles (NPs) either providing additional energy by heating their immediate surrounding [18] or generating and donating excited (hot) electrons and holes to the reacting species [13–16, 25–28]. In this respect, the injection of hot electrons (HEs) is a very efficient energetic process which allows to directly transfer an electron from the metal Fermi sea to the molecular excited state with an excitation energy lower than that required for a direct optical transition in the molecule. Such a process thus clearly extends the usable spectral range of solar radiation.

Chirality is pervasive in nature, from galactic to sub-molecular scale, going through small metabolites and amino acids to macromolecules such as proteins and DNA [29], The field of optics offers valuable tools to probe the chirality of nanosystems, including the measurement of circular dichroism (CD), the differential interaction strength between matter and circularly polarized light with opposite

helicity. Strong chiroptical responses are highly desirable capabilities for the realization of a wide range of applications, including circular polarizers, circular converters, polarization-encoded optical communication, polarization- selective chemical reactions, and localized heating [29].

According to recent studies [30–33], plasmonic chirality, as measured by CD, may be due to either structural chirality induced during the assembly of metallic nanoparticles (NPs) or plasmon-induced circular dichroism (PICD) of a chiral species [4–11]. In the former case, differences in circular dichroism can be observed as due to polydispersity in size or shape of the particles and presence of dihedral angles between the NPs in the assembly. In the case where particles are identical, spherical and perfectly monodisperse, CD signals can still originate from an achiral behavior based on the positional arrangement of the NPs, as found in Archimedean spirals. Recently, chiral plasmonic nanocrystals exhibiting large asymmetry factors in optical circular dichroism (CD), allowing for the generation of hot-electrons showing a very strong asymmetry, have been shown to provide mechanisms for chiral growth [12] and polarization-sensitive photochemistry [12, 21]. In the latter case, involving PICD of chiral molecules spatially and orientationally well-functionalized in the NPs' assembly, the presence of electromagnetic hotspots, generated by the proximity of metallic particles, constitutes the small chiral species' amplification mechanism [1, 2, 31].

In this paper, the large differential response to circularly polarized light created in the PICD process is shown to lead to a large asymmetric generation of hot electrons in the system, thereby being potentially able to induce a given chemical reaction. The model we will consider in order to describe the plasmon-induced chiral generation of hot electrons consists of two parts, naturally following the formal distinction between molecular plasmon-induced chiral effects [1, 2, 31] and injection of hot-electrons [22, 25]. In the first part, following Govorov et al. [1, 2, 31], we will distinguish between the optical response of a chiral plasmonic assembly, which is based on classical electrodynamics and the concept of plasmon-induced chirality. As the system we will further consider, chosen to be a dimer of "identical" gold NPs, is structurally achiral, a chirality being solely induced by the presence of a chiral molecule in the hotspot of the system, we will then consider the fields generated by the presence of this chiral molecule to calculate the asymmetric HEs injection rates according to the fundamental quantum-mechanical phenomenon of HE generation in plasmonic particles [21, 22, 25].

2. Results and Discussion

2.1. Chiroptical Response of a Plasmonic System

The extinction cross section σ_{ext} of an assembly of NPs quantifies the strength of its coupling with incident light. It is usually separated into the absorption σ_{abs} and scattering σ_{scat} components which pertain to two different types of light-matter interaction. While illuminated at their resonant frequencies, the interaction cross sections of noble metals (e.g., Au, Ag) nanostructures are much larger than their actual geometrical equivalents. Also, in case their dimensions are significantly smaller than the excitation wavelength (quasi-static approximation), σ_{scat} can generally be neglected, yielding

$$\sigma_{ext} = \sigma_{abs} + \sigma_{scat} \approx \sigma_{abs}$$

Such a cross-section σ_{abs} (m^2) is defined as the ratio of the power absorbed by the system Q_{abs} (W) to the incident energy flux I_0 (W/m^2):

$$\sigma_{abs} = \frac{Q_{abs}}{I_0}$$

for which

$$Q_{abs} = 2\omega\, Im(\varepsilon_m) \int dV\, \vec{E}_{tot}^2$$

and

$$I_0 = \frac{c_0}{\sqrt{\epsilon_s}} \left|\vec{E}_0\right|^2$$

where ε_m and ε_s are the dielectric constants of the metal and the surrounding environment, respectively, ω is the angular frequency of the incident light, and c_0 is the speed of light in vacuum. The vector $\vec{E}_{tot}$ is the complex electric field inside the metal and $\left|\vec{E}_0\right|$ denotes the field amplitude of the incident light.

The chiral optical activity, or circular dichroism, CD, is then determined from the optical cross sections of the system owing to the relation $CD \approx \Delta\sigma_{abs} = \sigma_{abs-} - \sigma_{abs+}$, where the subscripts - and + stand for Left Circularly Polarized and Right Circularly Polarized (RCP) light, respectively.

The formalism introduced so far is valid as long as the optical activity is generated by the structural chirality of a system. The LCP and RCP lights would then provide different excitations of the system, resulting in an observable CD signal. In this paper however, we aim to consider the case of a structurally achiral nanostructure and investigate the effect of a chiral molecule on the plasmon-induced circular dichroism (PICD) [1, 2, 31]. The simplest situation providing a significant amplification (plasmon-induced) process is the case of a dimer of gold NPs. In order to be sufficiently close to experimental situation, the Au cores are surrounded by a 1 nm shell of a dielectric medium with a relative permittivity (2.25) embedding the considered chiral molecule, L-Phe, and deposited on a substrate of AAO with an effective permittivity of 2.89. The whole system is then immerged in water. In order to clearly distinguish the effect of orientation of the molecule with respect to the gold surface, a single L-Phe molecule will be considered to be chirally active in the dielectric layer, with its electric dipole moment either normal or tangential to the Au surface, in the middle of the dimer axis. Figure 1 provides a scheme of the considered system.

According to the general quantum theory of optical activity, the strength of a molecular dipole's CD signal is given by $CD_0 \sim Im(\vec{\mu}_{12}.\vec{m}_{21})$ [34], where $\vec{\mu}_{12}$ and $\vec{m}_{21}$ are respectively the quantum matrix elements of the electric and magnetic dipole operators. The indices 1 and 2 denote the ground and excited states of the molecule. According to this equation, a molecule's CD signal arises from the joint reaction of its electric and magnetic dipoles to light.

Remarkably, in PICD [1, 2, 31], the chiral property (usually exhibited in the UV range) of a molecule can be both strongly enhanced and transferred to the visible wavelength range by using a plasmonic hot spot, here located in the middle of a nanoparticle dimer (Figure 1). By writing the total field as $\vec{E}_{tot} = \vec{E'} + \vec{E}_d$, where $\vec{E'}$ is mainly the field induced by the NPs in the absence of the molecule and $\vec{E}_d$ the field induced by the surface charge of the NPs, in turn induced by the molecule itself, Govorov et al. showed that the molecular circular dichroism of the molecular part could be written as $CD_{mol} = 2\omega_0\gamma_{21}((\sigma_{21}|^2_+ - (\sigma_{21}|^2_-)$, in the quasi-static limit, rotating wave approximation and using a perturbative approach for the quantum master equation of the molecule [1, 2, 31]. In this equation, ω_0 is the molecular transition frequency, γ_{12} is the damping from level 2 to level 1 and $\sigma_{21} = -\frac{\vec{\mu}_{21}.\vec{E'}+\vec{m}_{21}.\vec{B'}}{\hbar(\omega-\omega_0)+i\gamma_{21}-G}$, in which $G = -\vec{\mu}_{12}.\vec{E}_d$ at the position of the molecule.

In case a dimer of NPs is investigated, they further showed that the circular dichroism originating from the NPs could be separated into three parts $CD_{NP} = CD_{NP,ff} + CD_{NP,df} + CD_{NP,dd}$, where the three terms originate from the interaction of the $\vec{E'}$ and $\vec{E}_d$ vector fields in the following way: $CD_{NP,ff} = Q_{NP,ff+} - Q_{NP,ff-}$, where $Q_{NP,ff} = 2\omega\, Im(\varepsilon_{metal}) \int dV\, (\vec{E'}|^2$; $CD_{NP,df} = Q_{NP,df+} - Q_{NP,df-}$, where $Q_{NP,df} = 4\omega\, Im(\varepsilon_{metal})\, Re \int dV\, \vec{E}^*_d.\vec{E'}$ and $CD_{NP,dd} = Q_{NP,dd+} - Q_{NP,d-}$, where $Q_{NP,dd} = 2\omega\, Im(\varepsilon_{metal}) \int dV\, (\vec{E}_d|^2$. In all cases, the integration is performed on the volume of both NPs and $Q_{NP,ff}$, $Q_{NP,df}$ and $Q_{NP,dd}$ are thus the powers absorbed by the system, which have to be calculated in the - and + situations, e.g. for Left Circularly Polarized (LCP) and Right Circularly Polarized (RCP) excitation lights and then be subtracted. As a matter of fact, $CD_{NP,ff}$ will provide us with a zero contribution since the NP dimer system itself is non-chiral, so that two contributions remain for the NPs: $CD_{NPs}=CD_{NP,df}+CD_{NP,dd}$. In turn, the total circular dichroism potentially observable is $CD_{tot}=CD_{NP,df}+CD_{NP,dd}+CD_{mol}$.

In order to calculate the optical signals for this system, we performed Finite Difference Time Domain (FDTD) simulations [35]. We investigated 5 different configurations, e. g. gold spherical dimers with diameters ranging from 20 nm to 50 nm and surrounded by a 1 nm-thick shell of the L-Phe amino-acid (dielectric permittivity of 2.25), deposited on an AAO substrate (effective dielectric permittivity of 2.89), the whole system being immerged into water (dielectric permittivity of 1.8). In all simulations (Figure 1), an auto non-uniform mesh type with accuracy 6 has been used and the (Lumerical) Conformal Mesh Technology (CMT) was chosen, (the so-called conformal variant 0). To increase the accuracy and insure convergence, a sub-mesh with a step size of 1 nm was added in and immediately around the NPs. For the dielectric function of Au, Johnson and Christy's data have been chosen. Perfectly Matched Layers were implemented in all directions. For each configuration, two simulations have been performed, using either an electric dipole located in the middle of the dimer axis or a plane wave propagating backward while launched from the top of the structure, providing us with the $\vec{E}_d$ and $\vec{E'}$ fields required for the volume integrations.

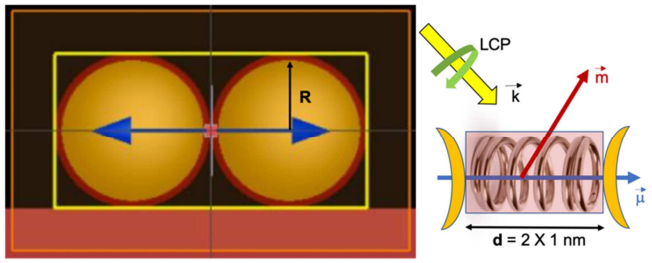

Figure 1. *Schematic of a chiral molecule in the hotspot of a gold spherical dimer. the NPs are surrounded by a 1 nm thick dielectric shell, deposited on an AAO substrate and the whole system is immerged in water.*

For the molecular dipole, we choose numbers typical for the experiments. The electric transition dipole moment is defined as: μ_{12}=|e| r_{12} and the magnetic one through the relation $\mu_{12}.m_{21}/\mu_{12}$=i |e| r_0 ω_0 r_{21} /2. In our calculations, we use r_{12}=0.2 nm, r_0=5.10^{-3} nm and γ_{12}=0.3 eV. The molecule (chosen to be L-Phe) has a resonance wavelength of 220 nm. The key chiral parameter r_0 determines the CD strength of the molecule $CD_{mol,0} \sim Im(\mu_{12}.m_{12}) \sim r_0$. This parameter is small since chirality of a molecule is usually weak. The above parameters of a chiral molecule yield typical numbers for the molecular extinction and CD [1, 2, 31]. Finally, for each configuration, we also have considered the molecular dipole to be oriented either parallel or perpendicular to the dimer axis.

2.1.1. Molecule's Electric Transition Dipole Moment Parallel to the Dimer Axis

Figure 2 shows the plasmon-induced circular dichroisms (PICDs) for the various investigated cases as one locate the chiral molecule in the center of the dimer axis, with its electric dipole moment parallel to the axis (e.g. perpendicular to the surfaces of the spheres). For each configuration, we show the dipole-field ($CD_{NP,df}$), dipole-dipole ($CD_{NP,dd}$), molecular (CD_{mol}) and total (CD_{tot}) contributions. The field-field contribution ($CD_{NP,ff}$) reduces to nullity because of structural symmetry.

By inspection of Figure 2, one obviously sees that, at the plasmon resonance, the dipole-field contribution gives the largest contribution to the observed PICD. Let us note here that the molecule itself does not absorb at the plasmon resonance. In such an off-resonant regime $\omega_0 - \omega_{pla} \gg \gamma_{12}, |G|$, the CD signal in the plasmonic band is proportional to the optical rotatory dispersion (ORD) $\frac{m_{12}.\mu_{12}}{\omega_0-\omega_{pla}}$ of the molecule [23]. The enhanced CD then originates from energy

dissipation inside metal NPs due to the joint action of the dipolar field of the chiral molecule (ORD response) and the external field. Since both dipolar and external fields are greatly enhanced in the vicinity of the hot spot, this dipole-field term shows a very strong enhancement. Concerning the molecular term, the function $G(\omega)$ and, accordingly, $CD_{NP,dd}$ play an essential role only for small distance d between the NPs, when the molecule-surface distance is small. $G(\omega)$ generates a broadening of the molecular resonance. As a consequence, the molecular CD band at 220 nm is transformed into an asymmetric profile (not shown) and the plasmonic CD profile becomes very strong and broad. The last effect, observable around and above 600 nm originates from the large enhancement of the electric field at the location of the chiral molecule and from Coulomb interaction between the chiral molecule and the achiral plasmonic nanostructure. Finally, the dipole-dipole term $CD_{NP,dd}$ appears due to the dissipation inside the metal cause by the molecular dipolar field.

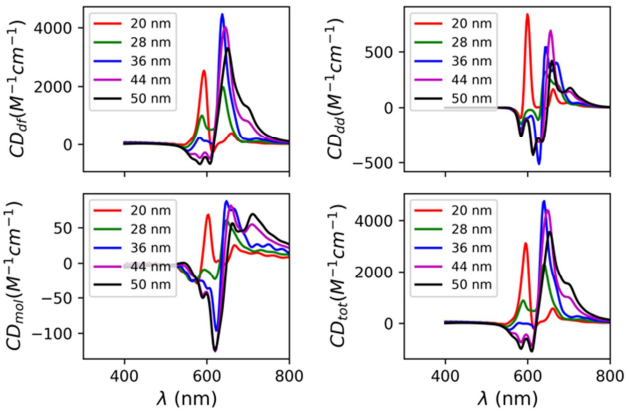

Figure 2. *Circular dichroism calculated for gold spherical dimers with core diameters ranging from 20 nm to 50 nm and comprising a molecule located in the middle of the dimer axis with its electric transition dipole moment oriented along the dimer axis.*

Figure 2 also shows that CD signals exhibit positive and negative contributions, which depend both on the direct environment and frequency. If one concentrates on the frequency giving the largest hot-spot enhancement, around a wavelength of 650 nm, one clearly observes that CD_{tot} increases, as a function of the spheres' diameters, up to 36 nm where it starts to saturate or even decrease if one goes further. This observation, which is best shown in Figure 5b, clearly is physically meaningful, since the leading dipole-field term, which describes the energy dissipation inside metal NPs due to the joint action of the dipolar field of a chiral molecule and the external field, increases as a function of volume up to a point where the combined action of the fields starts to vanish.

2.1.2. Molecule's Electric Transition Dipole Moment Perpendicular to the Dimer Axis

In case we locate the chiral molecule with its electric transition dipole moment oriented perpendicular to the dimer axis, e.g. tangentially to the surface of the NPs, as is often the case for an aromatic molecule simply adsorbed on a gold surface, one would assist to a completely different behavior (Figure 3).

All CD contributions exhibit a drastic decrease, by 3 orders of magnitude, as compared to the previous situation. As a matter of fact, this decrease originates, for each contribution, to a destructive interference between the fields involved in the volume integration. This configuration exemplifies the role of the environment, and in particular the simple and drastic effect of a change in molecular orientation of the chiral molecule. The maxima of the various CD signals do not appear clearly around 650 nm anymore. Furthermore, at this wavelength, CD_{tot} exhibits rather small magnitudes oscillating between positive and negative values as a function of the spheres' diameters as best observed in Figure 6b.

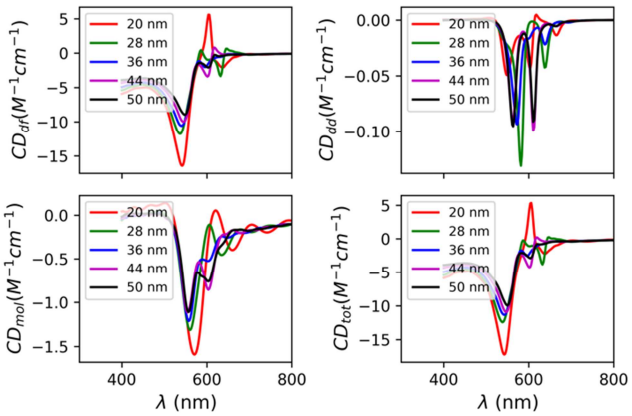

Figure 3. *Circular dichroism calculated for gold spherical dimers with core diameters ranging from 20 nm to 50 nm and comprising a molecule located in the middle of the dimer axis with its electric transition dipole moment oriented along the dimer axis.*

Based on these results, and leveraging on the clearly observed PICD effects, we now aim to investigate the potential strongly enhanced asymmetric generation and injection of HEs in the immediate surrounding of the NPs.

2.2. Generation of Hot Electrons in Chiral Systems

The photoexcitation process entails the absorption of a photon and the subsequent transition of an electron from the ground state to an excited state (Figure 4). During this process, two different types of excited electrons appear in the system [21, 36]. One is labeled "thermalized", the other "non-thermalized". The population of the latter cannot be described by the Fermi Dirac distribution since its distribution of electrons extends to energies well above the Fermi energy E_F, up to $E_F + \hbar\omega$. These so-called hot electrons (HEs) can directly be transferred to correctly aligned electronic states of molecules which would otherwise not be reachable by an internal transition of energy $\hbar\omega$, as Figure 4 schematically depicts. In such a case, the energy threshold is set so that the excited electron can overcome the energy barrier ΔE_b between the Fermi level E_F of the metal and the energy of the lowest unoccupied molecular orbital (LUMO).

The generation of nonthermal hot carriers being an ultrafast (100 fs) and nonequilibrium process, most HEs generated near the surface of a plasmonic nanostructure will be injected into its immediate surrounding, being able to perform chemical

reactions. In order to drive such reactions on time scales much larger than the typical lifetime of hot carriers inside the metal, a constant illumination might be used. Let us note that we set ΔE_b=0 in this paper, which has the effect to maximize the hot electron injection rates and allows us to draw conclusions with no particular consideration of a specific chemical reaction.

The solutions of the quantum master equation [8, 13–15, 17–21, 30, 36] treated in a perturbative approach provide a convenient way to quantify the rates of HE generation. Here is the final expression derived for these generation rates: $Rate_{HE} = \frac{2}{\pi^2}\frac{e^2E_F^2}{\hbar}\frac{1}{(\hbar\omega)^3}\int_S |E_n|^2\, ds$, where $E_n = E_\omega.\hat{n}$ is the electric field outgoing normally from a 1 nm distance of the inner surface (Figure 1) and S is the surface of the metal structure.

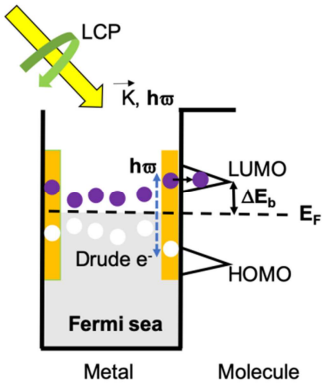

Figure 4. *Scheme of the energy diagram depicting optical excitation of electrons and holes inside the metal and their transfer to a neighboring molecule.*

Very importantly, this equation highlights that the excitation of HEs is a surface quantum effect, and it originates from the nonconservation of the electron's linear momentum due to its scattering by the surface.

Since we are interested in asymmetry of the HEs' generation, we will consider the difference between the LCP and RCP lights on the HE injection rates as $\Delta = Rate_{HE+} - Rate_{HE-}$, for which $\vec{E_{n\pm}} = \vec{E'_{\pm}} + \vec{E_{d\pm}}$, with the fields $\vec{E'_{\pm}}$ and $\vec{E_{d\pm}}$ being exactly the ones determined in the previous section, while the integration is now performed on the surface of the spheres.

Figure 5 shows the HEs injection rates difference (Δ) for the various systems of investigation consisting of dimers of gold NPs with 5 different diameters ranging from 20 to 50 nm. Here, the chiral molecule responsible for the chiral nature of the system is placed as usual in the middle of the dimer axis, with its electric transition dipole moment along the axis. HEs injected in the shell of the dimer system after + or – photoexcitation exhibit Δ which basically follows the trend of CD_{tot} (Figure 2) with a frequency modulation provided by the integrating quantum prefactor $(\hbar\omega)^{-3}$.

Figure 5a indeed shows wavelength-dependent HE rates' differences Δ with an increase of the generation rates as the size of the considered system increases. Again, if one follows the trend at a resonance wavelength of 650 nm, one observes clearly (Figure 5c) an increase of Δ followed by a saturation as one approaches a NP's size of 50 nm. The explanation of this behavior is multiple. Firstly, the integration on the surface area to release the generated HEs to the immediate surrounding medium plays a major role, increasing quadratically with the size of the NPs dimer. Secondly, the rates depend of course on the presence of plasmonic hot spots, which are especially strong in the gap region. Thirdly and finally, the HE generation rates include the quantum factor $(\hbar\omega)^{-3}$. This factor favors plasmon resonances in the red and IR. This is why the dimers with strong gap plasmons, which are typically in the near IR, are able to generate HEs so efficiently. When the size of the NPs increases, the gap-plasmon resonance shifts towards longer wavelength, which also involves a stronger quantum factor.

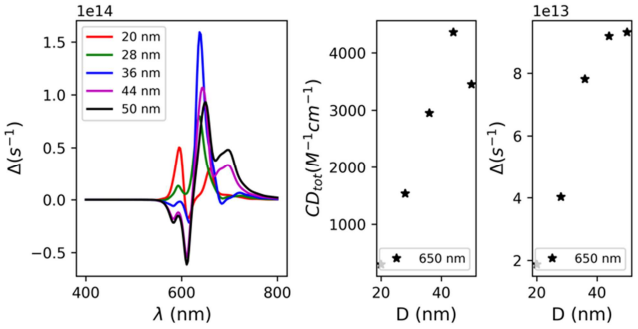

Figure 5. *Differences in HE injection rates between LCP and RCP photoexcited systems as a function of wavelength (a) and total CD signals (b) and rates' differences (c) observed as a function of the NPs' sizes. The chiral molecule has a transition dipole parallel to the dimer axis.*

In case the electric transition dipole moment of the chiral molecule lies parallel, tangential to the NPs' surfaces instead of perpendicular, one again assists to a completely different behavior with a drastic decrease, by 3 orders of magnitude, of the HE injections rates as shown in Figure 6.

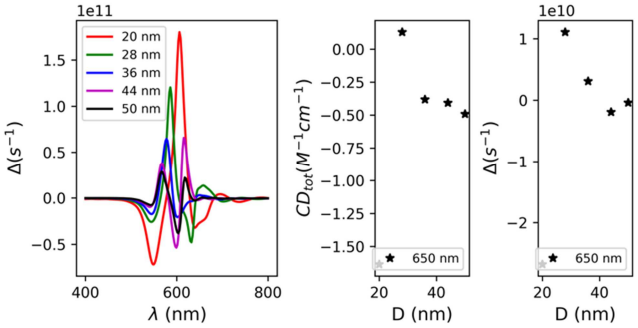

Figure 6. *Differences in HE injection rates between LCP and RCP photoexcited systems as a function of wavelength (a) and total CD signals (b) and rates' differences (c) observed as a function of the NPs' sizes. The chiral molecule has a transition dipole parallel to the dimer axis.*

This result highlights that, in order to provide strong asymmetric HEs injection in the immediate surrounding of the plasmonic NPs, as triggered by a chiral molecule, the latter must be oriented perpendicularly to the NPs' surfaces. This result closely follows the one obtained here above in the case of the plasmon-induced circular dichroism triggered by the very same chiral molecule. It also follows the usual trend of a maximum Raman scattering or maximum fluorescence

enhancement factor when the molecular species have their dipole moments oriented in a direction perpendicular to the NPs' surfaces. This trend, which is valid in the case of our NPs' dimers and also for a single plasmonic NP [31], might reveal more cumbersome to determine in complex NP assemblies [1].

On the experimental side, the situation is very challenging to accomplish, since fixing the location and orientation of a molecular species by functionalizing it close enough to a NP is a daunting task, even with the help of DNA technology [26–28, 37]. Furthermore, in order to obtain measurable signals, at least single layers of chiral molecules must be functionalized on the gold cores, with the orientation of the constituting dipoles fixed perpendicularly to the surface. Also, for the system to work as a "chiral" HEs' photoinjector able to perform chemical reactions, the reactive species must also lie in very close proximity of the NPs (order of 1 nm). All that set, our results clearly show that the PICDs (Δ) will scale up with the volume (surface) of the NPs, as far as the leading dipole-field term increases, e.g. as far as the combined action of the dipolar field of a chiral molecule and the external field starts to vanish (Figure 5 b, c), which corresponds to particle sizes of about 40 nm in the configuration here described.

3. Conclusion

In conclusion, by performing Finite Difference Time Domain simulations based on the combination of two models well-described in the literature, the simple design of an achiral gold NPs' dimer triggered by a chiral molecule located in the center and oriented with its transition electric dipole moment parallel to the dimer axis could is shown to be able to generate a strong asymmetry in its HEs' generation response. This asymmetry follows the general trend displayed by the plasmon-induced circular dichroism of the system triggered by the very same molecule. Both the asymmetric HEs' generation rate and the PICD are shown to be increasing functions of the NPs size, in volume and in surface respectively, up to a saturation level determined by the combined action of the dipole and external fields, keeping the separation between the NPs constant. Such calculations might prove very useful to initiate experimental studies of polarization-dependent surface reactions with bottom-up engineering techniques which might prove easier and produced at larger scales as compared to the synthesis of chiral structures.

References

[1] Alexander O. Govorov "Plasmon-Induced Circular Dichroism of a Chiral Molecule in the Vicinity of Metal Nanocrystals. Application to Various Geometries". Journal of Physical Chemistry C, 115 (16): 7914–7923, 2011.

[2] Alexander O. Govorov and Zhiyuan Fan "Theory of chiral plasmonic nanostructures comprising metal nanocrystals and chiral molecular media.". Chem Phys Chem, 13 (10): 2551–2560, 2012.

[3] Wenhe Wang, Fengxia Wu, Yanqun Zhang, Wenli Wei, Wenxin Niu, Guobao Xu, and Guobao Xu "Boosting Chiral Amplification in Plasmon-Coupled Circular Dichroism Using Discrete Silver Nanorods as Amplifiers". Chemical Communications, 57: 7390–7393, 2021.

[4] Yun Wen, Meng-Qi He, Yong-Liang Yu, and Jian-Hua Wang "Biomolecule mediated chiral nanostructures a review of chiral mechanism and application". Advances in Colloid and Interface Science, 289: 102376, 2021.

[5] Zhijian Hu, Dejing Meng, Feng Lin, Feng Lin, Xing Zhu, Zheyu Fang, and Xiaochun Wu "Plasmonic Circular Dichroism of Gold Nanoparticle Based Nanostructures". Advanced Optical Materials, 7 (10): 1801590, 2019.

[6] Lucas V. Besteiro, Hui Zhang, Hui Zhang, Jérôme Plain, Gil Markovich, Zhiming Wang, Zhiming Wang, and Alexander O. Govorov "Aluminum Nanoparticles with Hot Spots for Plasmon-Induced Circular Dichroism of Chiral Molecules in the UV Spectral Interval". Advanced Optical Materials, 5 (16): 1700069, 2017.

[7] Ben M. Maoz, Yulia Chaikin, Alexander B. Tesler, Omri Bar Elli, Zhiyuan Fan, Alexander O. Govorov, and Gil Markovich "Amplification of chiroptical activity of chiral biomolecules by surface plasmons." Nano Letters, 13 (3): 1203–1209, 2013.

[8] H Atwater and A Polman "Plasmonics for improved photovoltaic devices". Nature Mater, 9: 205–213, 2010.

[9] C Clavero "Plasmon-induced hot-electron generation at nanoparticle/metal-oxide interfaces for photovoltaic and photocatalytic devices". Nature Photon, 8: 95–103, 2014.

[10] Scott K. Cushing and Nianqiang Wu "Progress and Perspectives of Plasmon-Enhanced Solar Energy Conversion". The Journal of Physical Chemistry Letters, 7 (4): 666–675, 2016.

[11] Narima Eerqing, Aneeth Kakkanattu, Aneeth Kakkanattu, Shahin Ghamari, and Frank Vollmer "Review of optical sensing and manipulation of chiral molecules and nanostructures with focus on plasmonic enhancements". Optics Express, 29 (8): 12543–12579, 2021.

[12] Larousse Khosravi Khorashad, Lucas V. Besteiro, Miguel A. Correa-Duarte, Sven Burger, Zhiming Wang, and Alexander O. Govorov "Hot Electrons Generated in Chiral Plasmonic Nanocrystals as a Mechanism for Surface Photochemistry and Chiral Growth.". Journal of the American Chemical Society, 142 (9): 4193–4205, 2020.

[13] Mark L. Brongersma, Naomi J. Halas, and Peter Nordlander "Plasmon-induced hot carrier science and technology". Nature Nanotechnology, 10: 25–34, 2015.

[14] Kaifeng Wu, Jacqueline Chen, James R Mcbride, and Tianquan Lian "Efficient hot electron transfer by a plasmon induced interfacial charge transfer transition". Science, 349: 632–635, 2015.

[15] Linan Zhou, Dayne F. Swearer, Chao Zhang, Chao Zhang, Hossein Robatjazi, Hangqi Zhao, Luke Hen- derson, Luke C. Henderson, Liangliang Dong, Phillip Christopher, Emily A. Carter, Peter Nordlander, and Naomi J. Halas "Quantifying hot carrier and thermal contributions in plasmonic photocatalysis". Science, 362 (72): 69, 2018.

[16] Yuchao Zhang, Shuai He, Shuai He, Wenxiao Guo, Yue Hu, Jiawei Huang, Jiawei Huang, Jiawei Huang, Justin R. Mulcahy, and Wei David Wei "Surface-Plasmon-Driven Hot Electron Photochemistry". Chemical Reviews, 118 (6): 2927–2954, 2017.

[17] Yisong Zhu, Hongxing Xu, Peng Yu, and Zhiming Wang "Engineering plasmonic hot carrier dynamics toward efficient photodetection". Applied physics reviews, 8: 021305, 2021.

[18] Calum Jack, Affar S. Karimullah, Ryan Tullius, Larousse Khosravi Khorashad, Marion Rodier, Brian Fitzpatrick, Laurence D. Barron, Nikolaj Gadegaard, Adrian J. Lapthorn, Vincent M. Rotello, Graeme Cooke, Alexander O. Govorov, and Malcolm Kadodwala "Spatial control of chemical processes on nanostructures through nanolocalized water heating.". Nature Communications, 7: 10946, 2016.

[19] Xu Shi, Kosei Ueno, Tomoya Oshikiri, Quan Sun, Keiji Sasaki, Hiroaki Misawa, Hiroaki Misawa, Hiroaki Misawa, and Hiroaki Misawa "Enhanced water splitting under modal strong coupling conditions". Nature Nanotechnology, 13: 953–958, 2018.

[20] Shaunak Mukherjee, Florian Libisch, Nicolas Large, Oara Neumann, Lisa V. Brown, Jin Cheng, J. Britt Lassiter, Emily A. Carter, Peter Nordlander, and Naomi J. Halas "Hot Electrons Do the Impossible: Plasmon- Induced Dissociation of H2 on Au". Nano Letters, 13 (1): 240–247, 2013.

[21] Tianji Liu, Lucas V. Besteiro, Tim Liedl, Miguel A. Correa-Duarte, Zhiming Wang, and Alexander O. Govorov "Chiral Plasmonic Nanocrystals for Generation of Hot Electrons: Toward Polarization-Sensitive Photochemistry.". Nano Letters, 19 (2): 1395–1407, 2019.

[22] Alexander O. Govorov, Hui Zhang, Hui Zhang, and Yurii K. Gun'ko "Theory of Photoinjection of Hot Plasmonic Carriers from Metal Nanostructures into Semiconductors and Surface Molecules". Journal of Physical Chemistry C, 117 (32): 16616–16631, 2013.

[23] Hui Zhang, Hui Zhang, and Alexander O. Govorov "Giant circular dichroism of a molecule in a region of strong plasmon resonances between two neighboring gold nanocrystals". Physical Review B 87: 075410, 2013.

[24] Huilei Zhao, Xiaoyu Zheng, Xuhui Feng, and Ying Li "CO_2 Reduction by Plasmonic Au Nanoparticle- Decorated TiO_2 Photocatalyst with an Ultrathin Al2O3 Interlayer". Journal of Physical Chemistry C, 122 (33): 18949–18956, 2018.

[25] Lucas V. Besteiro, Xiang-Tian Kong, Zhiming Wang, and Alexander O. Govorov. Theory of Plasmonic Excitations: Fundamentals and Applications in Photocatalysis. WILEY-VCH GmbH, 2021.

[26] Vivek V. Thacker, Lars O. Herrmann, Daniel O. Sigle, Tao Zhang, Tao Zhang, Tao Zhang, Tim Liedl, Jeremy J. Baumberg, and Ulrich F. Keyser "DNA origami-based assembly of gold nanoparticle dimers for surface-enhanced Raman scattering". Nature Communications, 5: 3448, 2014.

[27] Suchetan Pal, Zhengtao Deng, Baoquan Ding, Hao Yan, and Yan Liu "DNA-Origami-Directed Self-Assembly of Discrete Silver-Nanoparticle Architectures". Angewandte Chemie, 49 (15): 2700–2704, 2010.

[28] Anastasiya Puchkova, Carolin Vietz, Enrico Pibiri, Bettina Wünsch, Maria Sanz Paz, Guillermo P. Acuna, and Philip Tinnefeld "DNA Origami Nanoantennas with over 5000-fold Fluorescence Enhancement and Single- Molecule Detection at 25 μM.". Nano Letters, 2015.

[29] X. T Kong, L V Besteiro, Z Wang, and A O Govorov "Plasmonic Chirality and Circular Dichroism in Bioassembled and Nonbiological Systems: Theoretical Background and Recent Progress". Adv. Mater, 32: 1801790–1801790, 2020.

[30] Xiang-Tian Kong, Lucas V. Besteiro, Zhiming Wang, and Alexander O. Govorov "Plasmonic Chirality and Circular Dichroism in Bioassembled and Nonbiological Systems: Theoretical Background and Recent Progress.". Advanced Materials, 32 (41): 1801790, 2018.

[31] Alexander O. Govorov, Zhiyuan Fan, Pedro Hernandez, Joseph M. Slocik, and Rajesh R. Naik "Theory of Circular Dichroism of Nanomaterials Comprising Chiral Molecules and Nanocrystals: Plasmon Enhancement, Dipole Interactions, and Dielectric Effects". Nano Letters, 10 (4): 1374–1382, 2010.

[32] Maximilian J. Urban, Chenqi Shen, Xiang-Tian Kong, Chenggan Zhu, Alexander O. Govorov, Qiangbin Wang, Mario Hentschel, and Na Liu "Chiral Plasmonic Nanostructures Enabled by Bottom-Up Approaches.". Annual Review of Physical Chemistry, 70 (1): 275–299, 2019.

[33] Qihui Ye, Q. H. Ye, Xudong Chen, X. D. Chen, Shihong Wang, Shijie Wang, Z. Y. Hu, Gang Song, and G. Song "Chirality-detecting–based chiral molecule-metal-chiral molecule structures". EPL, 134: 27003, 2021.

[34] Robert W. Woody. Theory of Circular Dichroism of Proteins. In G. D. Fasman, editor, Circular Dichroism and the conformational analysis of biomolecules, pages 25–67, New York, 1996. Plenum.

[35] Lumerical Inc.

[36] Lucas V. Besteiro and Alexander O. Govorov "Amplified Generation of Hot Electrons and Quantum Surface Effects in Nanoparticle Dimers with Plasmonic Hot Spots". Journal of Physical Chemistry C, 120 (34): 19329–19339, 2016.

[37] Anton Kuzyk, Ralf Jungmann, Guillermo P. Acuna, and Na Liu "DNA Origami Route for Nanophotonics". ACS Photonics, 5 (4): 1151–1163, 2018.